DENSITY FUNCTIONAL THEORY AND DOCKING OF POLYANILINE WITH SARS-CoV-2

A. Ananda Jebakumar[1], P. Sumithraj Premkumar[2], J. Ilavarasi Jeyamalar[3] and C. Ravi Samuel Raj[3*]

[1]Department of Chemistry, Government Polytechnic College for Women, Madurai, Tamilnadu, India-625 011

[2]Department of Physics, St. John's College, Palayamkottai, Tirunelveli district, Tamilnadu, India – 627002

[3]Department of Chemistry, Pope's College (Autonomous), Sawyerpuram, Thoothukudi district, Tamilnadu, India - 628251

*ravisamuelraj@gmail.com

Abstract

Polymer based drug delivery is advancing in recent years. Among natural polymers synthetic polymers also having the drug delivering properties. Polyamine (PANI) is an important conducting polymer and have proven antimicrobial activities. Computational method provide accurate details about the chemical behaviour, in this regard DFT is an important method. DFT studies were performed by B3LYP/6-31G** basis set in the gas phase at 25 °C using firefly software and docking were done by Auto Dock. This work is to analyse the behaviour of PANI derivatives for the chemistry behind this. To prove the drug delivering behaviour their docking studies were performed for SARS-CoV-2-7N0R. In order to get the clear understanding about the behaviour of PANI its starting aniline (AN), aniline hydrochloride (ANHC), emeraldine base (EB) and emaraldine salt (ES) with two units of phenylene rings were studied. It has been concluded that PANI is more stable and can effectively deliver the drug in the specific site by its mobile HCl.

Keywords: PANI, DFT, docking studies, SARS-CoV-2-7N0R

1. Introduction

Polymer based drug design is alarming due to their intense applications [1]. This involves multi-disciplinary approaches through computer base quantum mechanical modeling, docking, synthesis, characterisation and application to the specific target [2]. Polymeric drug delivery is a formulation or a device that enables the introduction of a therapeutic substance into the body [3]. This systems can specifically targeting the area and deliver the drug specifically. Conducting polymers have considerable attention due to their electronic properties [4]. Among them polyaniline (PANI) has studied extensively due to their tunable oxidation state and degree of doping [5]. PANI also has good environmental stability and economically feasible [6]. PANI can be easily synthesized chemically as well as electrochemically [7]. PANI-composites have antifungal and antibacterial activities [8]. Dye substituted PANI control bacterial and fungal strains [9]. PANI doped ortho phosphoric showed higher antimicrobial activity compared to ortho phosphoric acid [10]. Lower concentrations of PANI strongly inhibited the growth of *Escherichia coli, Pseudomonas aeruginosa* and *Staphylococcus aureus* as well as several antibiotic-resistant clinical pathogens [11]. PANI-Zr (IV) sulphosalicylate can inhibit the bacterial *E. col*i, *B. thuringiensis* and *P. aeruginosa* and fungal strains *A. niger*, *F. oxysporum* and *P. chrysogenum* with relatively higher activities over genrally known antibiotics [12]. Grafting of chitosan in polyaniline improve its properties like chelation, complexation, adsorption and biocidal activity. PANI grafted chitosan has antimicrobial activity against *S. epidermidis*, *S. aureus*, *S. pyogenes*, *E. coli*, *C. albicans*, *C. tropicalis* and *C. krusei* [13]. Dye substituted PANI possesses good biocidal activities as compared to acid-doped PANI or dye alone [14]. The higher activity of PANI is due to its redox nature, crystallinity, and simple protonation of the imine nitrogen atoms in the emeraldine base backbone gives PANI and enhance its properties [15]. Molecular modelling has

3989

emerged as a viable and powerful approach to chemistry problems. These methods are used in lieu of tactile model to visualise molecular shapes, electronic properties, steric effects and reaction energies with sufficient accuracy to support experiments. Among the computational methods, density functional theory (DFT) of electronic structure has made an unparalleled impact on the application of quantum mechanics to interesting and challenging problems in chemistry [16]. This work is to analyse the behaviour of aniline derivative, PANI by DFT and docking towards SARS-CoV-2-7N0R. To get the depth understanding about PANI aniline (AN), aniline hydrochloride (ANHC), emeraldine base (EB) and emaraldine salt (ES) which is the computational model for PANI with two units of phenylene rings.
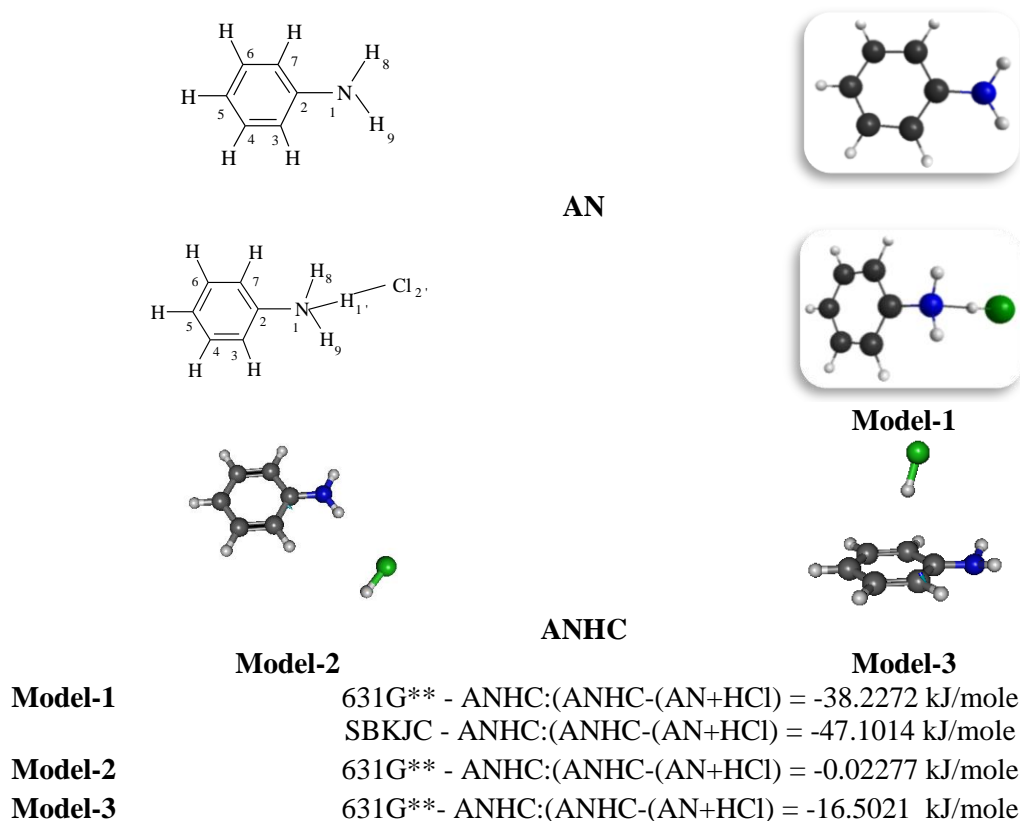
2. Materials and Method

DFT studies were performed by B3LYP/6-31G** basis set in the gas phase at 25 °C using firefly software [17] in i7 computer. Due to higher computational cost, the modeling studies were carried for each one unit of phenyl and phenylene rings for PANI. Docking were done through Auto Dock [18].
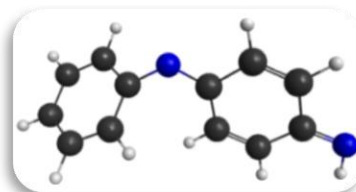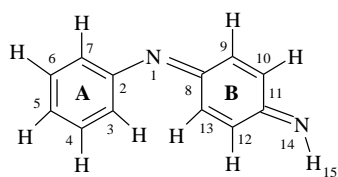
3. Results and Discussion

3.1 Stability and Structure

Details about the stability and structure are given in Fig 1. ES mimics ANHC in many respects so the latter is studied thoroughly. ANHC is the protonated form of AN. In general AN is much weaker base than aliphatic amines and this can be attributed to a combination of inductive effect from the more electronegative sp^2 carbon and resonance effects, as the lone pair on the nitrogen is partially delocalized into the π-system of the

Figure 1: Structure and Thermodynamic Stability

AN

Model-1

ANHC

Model-2   Model-3

Model-1	631G** - ANHC:(ANHC-(AN+HCl) = -38.2272 kJ/mole
	SBKJC - ANHC:(ANHC-(AN+HCl) = -47.1014 kJ/mole
Model-2	631G** - ANHC:(ANHC-(AN+HCl) = -0.02277 kJ/mole
Model-3	631G**- ANHC:(ANHC-(AN+HCl) = -16.5021 kJ/mole

EB

631G**- EB:(EB-((2* AN)-2*H_2)) = 271.3979 kJ/mole
SBKJC-EB:(EB-((2* AN)-2*H_2)) = 303.685 kJ/mole
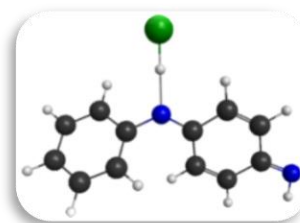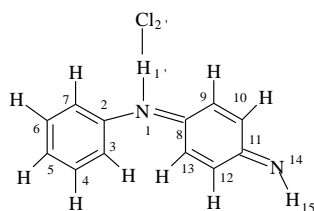
ES

ES:(ES-(((2* AN)-2*H_2)+HCl) = 230.2038 kJ/mole

631G**   ES:(ES-(EB+HCl) = -41.1941 kJ/mole Charge=0, Multi=1
ES:(ES-(EB+HCl) = 63.1433 kJ/mole Charge=0, Multi=3
ES:(ES-(EB+HCl) = 690.375 kJ/mole Charge=+1, Multi=2
SBKJC   ES:(ES-(EB+HCl) = -80.3403 kJ/mole

C-Black; H-White; N-Blue; Cl-Green benzene ring. AN is more basic than ammonia in the gas phase, but ten thousand times less so in aqueous solution.

Three structures of ANHC were fully optimised. In Model-I AN and HCl are one H-bond acceptor and donor, here the acceptor is nitrogen and donor is chloride atom respectively. Model-II, both AN and HCl are two H-bond donor and acceptor, in which acceptor is chloride and donor is nitrogen. Model-III, AN is single acceptor and HCl is single donor, the receptor is π-electron cloud of benzene ring and chloride is the donor. The thermodynamic stability of the three models suggest that Model-I is more stable and Model-II is the least stable. This result indicates that HCl of ANHC is mobile and moves through the whole volume of AN at room temperature. For further studies Model-I is chosen due to its higher stability over other models. In general the reaction between AN and HCl is considered as proton transfer neutralisation reaction. Neutralisation reactions are exothermic in nature. The above evidence is true for this reaction, as the computed stability of ANHC is higher than the sum of stabilities of AN and HCl. Thus, this gas phase reaction between AN and HCl is an equilibrium neutralisation reaction at room temperature and the equilibrium shifts to the right as

$$AN+HCl \rightleftharpoons ANHC$$
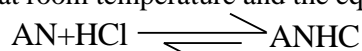
ES is the polymeric form of ANHC. The stability order of ES in different multiplicities and charges is; ES (Charge=0; Mult=1) > ES (Charge=0; Mult=3) > ES (Charge=1; Mult=2). Thus, ES (Charge = 0; Multiplicity =1) is taken for further studies.

The protonated form of EB is ES and the stability of EB is less than ANHC and ES. Like the previous reaction, among AN and HCl, the reaction between EB and HCl is reversible neutralisation reaction inclined to the right can be represented as

$$EB+HCl \rightleftharpoons ES$$
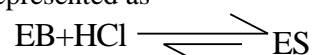
The higher stability of ES over EB may leads to the conductance of ES. The protonation enhanced the stability of both monomer (AN) and polymer (EB) and this may be due to the difference in the resonance stabilisation of the electron deficiency and change in the geometry caused by the protonation. The order of stability is (% increase from ANHC) ES (8%) > ANHC

Structure

　　　　Structural parameters are given in Table 1. The structural parameters are bond lengths, bond angles and dihedral angles. Due to space and time important geometrical parameters are discussed.

Table 1: Structural Parameters

EB

Atom Pair	Bond Length (Å)	Atom Pair	Bond Angle (°)	Atom Pair	Dihedral Angle (°)
N_1-C_2	1.3985	N_1-C_2-C_7	117.764	N_1-C_2-C_7-C_6	-177.26
N_1-C_8	1.2981	C_2-C_3-C_4	120.285	C_2-N_1-C_8-C_{13}	8.53
C_2-C_3	1.4090	C_3-C_4-C_5	120.512	C_3-C_2-C_7-C_6	-2.82
C_2-C_7	1.4078	C_4-C_5-C_6	119.488	C_3-C_4-C_5-C_6	-1.21
C_3-C_4	1.3941	C_5-C_6-C_7	120.425	C_4-C_5-C_6-C_7	-0.30
C_4-C_5	1.3955	C_6-C_7-C_2	120.477	C_5-C_6-C_7-C_2	2.33
C_5-C_6	1.3983	C_7-C_2-C_3	118.753	C_7-C_2-N_1-C_8	-134.30
C_6-C_7	1.3907	C_8-N_1-C_2	123.671	C_9-C_{10}-C_{11}-C_{12}	1.05
C_8-C_{13}	1.4707	C_9-C_{10}-C_{11}	121.576	C_{10}-C_{11}-C_{12}-C_{13}	-2.15
C_9-C_{10}	1.3466	C_{10}-C_{11}-C_{12}	116.321	C_{11}-C_{12}-C_{13}-C_8	0.58
C_{10}-C_{11}	1.4674	C_{11}-C_{12}-C_{13}	122.199	C_{12}-C_{13}-C_8-N_1	179.67
C_{11}-C_{12}	1.4714	C_{12}-C_{13}-C_8	121.130	N_{14}-C_{11}-C_{12}-C_{13}	178.89
C_{11}-N_{14}	1.2917	C_{13}-C_8-N_1	126.306	H_{15}-N_{14}-C_{11}-C_{12}	-0.77
C_{12}-C_{13}	1.3477	N_{14}-C_{11}-C_{12}	125.035		
N_{14}-H_{15}	1.0261	H_{15}-N_{14}-C_{11}	110.035		

ES

Atom Pair	Bond Length (Å)	Atom Pair	Bond Angle (°)	Atom Pair	Dihedral Angle(°)
$H_{1'}$-$Cl_{2'}$	1.3743	$Cl_{2'}$-$H_{1'}$-N_1	178.00	$Cl_{2'}$-$H_{1'}$-N_1-C_8	-82.78
$H_{1'}$-N_1	1.6195	$H_{1'}$-N_1-C_2	114.52	$H_{1'}$-N_1-C_2-C_7	40.56
N_1-C_2	1.4056	$H_{1'}$-N_1-C_8	120.36	$H_{1'}$-N_1-C_8-C_9	8.69
N_1-C_8	1.3037	N_1-C_2-C_7	117.54	N_1-C_2-C_7-C_6	-177.76
C_2-C_3	1.4072	C_2-C_3-C_4	120.02	C_2-N_1-C_8-C_{13}	8.43
C_2-C_7	1.4062	C_3-C_4-C_5	120.41	C_3-C_2-C_7-C_6	-2.99
C_3-C_4	1.3934	C_5-C_6-C_7	120.43	C_3-C_4-C_5-C_6	-1.23
C_4-C_5	1.3959	C_6-C_7-C_2	120.07	C_4-C_3-C_2-C_7	2.00
C_5-C_6	1.3976	C_7-C_2-C_3	119.34	C_5-C_6-C_7-C_2	1.89
C_6-C_7	1.3912	C_8-N_1-C_2	125.09	C_8-N_1-C_2-C_7	-137.12

C_8-C_{13}	1.4675	$C_9-C_{10}-C_{11}$	121.80	$C_9-C_{10}-C_{11}-C_{12}$	1.59
C_9-C_{10}	1.3469	$C_{10}-C_{11}-C_{12}$	116.38	$C_{10}-C_{11}-C_{12}-C_{13}$	-2.68
$C_{10}-C_{11}$	1.4669	$C_{11}-C_{12}-C_{13}$	122.07	$C_{11}-C_{12}-C_{13}-C_8$	0.00
$C_{11}-C_{12}$	1.4709	$C_{12}-C_{13}-C_8$	120.91	$C_{12}-C_{13}-C_8-N_1$	-180.00
$C_{11}-N_{14}$	1.2909	$C_{13}-C_8-N_1$	125.13	$N_{14}-C_{11}-C_{12}-C_{13}$	178.47
$C_{12}-C_{13}$	1.3477	$N_{14}-C_{11}-C_{12}$	125.03	$H_{15}-N_{14}-C_{11}-C_{12}$	-0.87
$N_{14}-H_{15}$	1.0261	$H_{15}-N_{14}-C_{11}$	110.28		

Bond Length

Distance between the atomic centres of bonded atoms in a molecule is bond length, which gives the information about electron density and strength between interacting atoms. Bond length may vary depending on many factors, but in general they are very consistent and ranges from 0.74 Å to 2.0 Å. Of course the bond order affects bond length, but bond lengths of the same order for the same pair of atoms in various molecules are comparable.

$H_{1'}-Cl_{2'}$ bond

Hydrogen chloride has polar covalent bond and its weaker dipole-dipole interaction than water is due to bigger size of chloride over oxygen. Hydrogen chloride is anhydrous gaseous form and hydrochloric acid is aqueous solution of hydrogen chloride gas. $H_{1'}-Cl_{2'}$ bond length of ES is 0.7, 8.2, 6.9 and 2.3 percentage higher than bond length calculated from covalent radii, literature, computed and ANHC. Usually the polar covalent bonds are shorter than the sum of covalent radii. When two oppositely charged ions approach each other the positive ion attracts electron on the outermost shell of the anion and repels its positively charged nucleus. This results in the distortion, deformation or polarisation of anion. If the polarisation is quite small, an ionic bond is formed. Thus, the study reveals that the $H_{1'}-Cl_{2'}$ in ES has more covalent character, further its interaction with EB polarised $Cl_{2'}$ in a greater extent than hydrochloric acid. Like ANHC the $H_{1'}-Cl_{2'}$ in ES diffused over the π-electron cloud of the benzene ring and the nitrogen atoms. Finally, it may be concluded that the reaction between EB and HCl is neutralisation and not protonation in gas phase.

N-H Bonds

In this work N-H bonds with two different bond lengths are observed for hydrogen atom covalently linked to the nitrogen atom and protonated hydrogen. Depends on the degree of protonation the N-H bond length varies from 0.86 to 1.14 Å. If the bond length is shorter, the degree of protonation is higher. The two N-H bonds are, $N_1-H_{1'}$ and $N_{14}-H_{15}$.   The $N_1-H_{1'}$ bond measures the impact of protonation on N_1. This bond in ES is 28.4, 39.2, 39 and 38.4 percentage higher than covalent radii of N-H single bond, experimental value of N-H single bond, computed N_1-H_8 bond in AN and ANHC. Further it is 19.7 % less than the computed $N_1-H_{1'}$ bond length of ANHC. This indicates that the protonation in EB is approximately 20% stronger than AN. Therefore $H_{1'}-Cl_{2'}$ in ES has neutralisation reaction along with protonation of 20% (quasi-doping) higher strength than the protonation on AN. Due to the quasi-doping effect of $H_{1'}-Cl_{2'}$ on EB enhance the ability of electrons to move from one end of the polymer to the other through the extended *p*-orbital system. It has been concluded that the counter ion, chloride plays a major role in the conductive behaviour of ES. The $N_{14}-N_{15}$ bond in ES is no and minor deviation from EB and literature. Thus, $N_{14}-N_{15}$ bond is not significantly affected by quasi-protonation on EB.

N-C Bonds

The N_1-C_2 bond length of ES is 4.4 % less than C-N single bond and respectively 5.1 and 9 % higher than C-N aromatic and C=N bond lengths. This implies that the N_1-C_2 bond has partial double bond character. The N_1-C_2 bond length of ES is dilated than AN and this may be attributed for the quasi-protonation effect in the former. Further the above bond length in ES is lesser than ANHC and can be explained as the proton is accommodated by ES much in ease when compared to ANHC. The

other two C-N bonds such as N_1-C_8 and C_{11}-N_{14} has less than 2% deviation from the standard C=N bond length. The low alteration in the bond lengths suggest that there is no significant Peierl's distortion in ES. The bridging atom N_1 transfers the resonating effect more on electron rich benzenoid over quinoid structure. The N_1-$H_{1'}$, N_1-C_2, and $H_{1'}$-$Cl_{2'}$ bonds in ES are altered significantly with the order N_1-$C_2 < N_1$-$H_{1'} < H_{1'}$-$Cl_{2'}$. Based on bond lengths, it has been concluded that the impact of $H_{1'}$-$Cl_{2'}$ on EB is less and vice versa.

Bond Angle

Next to bond length, bond angle is an important geometrical parameter which explains the orientation of atoms in a molecule.

N_1-$H_{1'}$-$Cl_{2'}$

The above bond angle for ES is almost 180° and increased from ANHC by 0.5 %. This implies that attack of $H_{1'}$-$Cl_{2'}$ on N_1 takes place in a same plane and the planarity is caused by sp^2 hybridisation of N_1.

$H_{1'}$- N_1-C_2

This parameter in ES indicates the protonation angle of $H_{1'}$ with respect to EB. It is 4.6% less than the standard sp^2 hybridisation and 63.3 and 1.4% greater than standard sp^3 hybridisation and ANHC respectively. As a result the interaction between $H_{1'}$ and N_1 does not alters the hybridisation of N_1. For that reason $H_{1'}$ -N_1 is quasi-protonated bond.

C_2-N_1-C_8

The above bond angle measures the angle between benzenoid and quinonoid rings and it is 3.1 and 4.2 % higher than the standard sp^2 angle respectively for EB and ES. Carbon has two principle structures, diamond and graphite. The sp^3 hybridisation has strong and rigid structure while in sp^2 hybridisation three electrons from the back bone and the π-electron highly delocalised due to less electron-electron interaction. The distortion in the bond lengths and bond angles can be explained by VSEPR theory as the $H_{1'}$ forms a primary bond with Cl_2' and a secondary bond with the lone pair of N_1 and their by making ES as a resonance hybrid with delocalised lone pair, which account for the higher conducting ability of ES over EB through percolation effect. Further the inter-chain bonds are weaker than intra-chain bonds in EB over ES and accounts for the latter's conducting ability.

Dihedral Angle

Dihedral angle is a measure of twist between atoms or groups in a molecule. It provides information about conformations around rotatable bonds and attacking atom or group on the substrate. Dihedral $Cl_{2'}$-$H_{1'}$-N_1-C_2 gives information about the plane of approach of $H_{1'}$-$Cl_{2'}$ with N_1. In ANHC, $H_{1'}$-$Cl_{2'}$ approaches N_1 in planar mode while, ES has angular approach from the top or bottom of N_1 with a percentage decrease by 52.1 from ANHC. The planar approach in ANHC is due to π-electron cloud of benzene which blocks the top/bottom approach. The top/bottom approach for ES and deviation from exact perpendicular is due to steric and VSEPR effects caused by the two rings and N_1. The twist angle between ring A and ring B with $H_{1'}$ is 40.56° and 8.69° respectively for ES. Only 0.1° difference between ring A and ring B is observed in the twist angle for EB and ES. This result indicates that the rings are almost planar and the twist angle may be due to single and double bond character of N_1-C_2 and N_1-C_8. The dihedral angle is very low and ES may have free rotation along N_1-C_2 due to low barrier.

3.2 Charge Density

Table 2 has the values of charge density. Chemistry is more are less the electron behaviour and at this juncture it emphasis the electronic effect. Charge density gives the information about the population of electron in a atom within the molecule. It is a measure of localisation and delocalisation of electron cloud around the atom. Charge density on $H_{1'}$ of ES is 0.9% higher than $H_{1'}$-$Cl_{2'}$ and only negligible increase for ANHC. This suggests that $H_{1'}$ of ES is slightly oxidised than in $H_{1'}$-$Cl_{2'}$. This may be due to the H-bond formation between N_1- $H_{1'}$-$Cl_{2'}$. Charge on H_{15} of ES is 2.8% higher than EB, shows that the delocalisation of electrons in ES is higher than EB and explains the conducting behaviour of the former.

Charge Density on $Cl_{2'}$

Atomic charge density on $Cl_{2'}$ of ANHC and ES are 60.4 and 75.4% higher than that of $H_{1'}$-$Cl_{2'}$. Preceding results suggest that the $Cl_{2'}$ has relatively gained charge from the phenyl group and the polymer chain through $H_{1'}$. Here, acquisition of charge by $Cl_{2'}$ may increase the density of states for a quantum well created between $Cl_{2'}$ and polymer back bone, through quantum field effect enhancing the hoping drift velocity of $H_{1'}$. This leads to the steep raise in the conductance of ES over EB.

Table 2: Mulliken's Atomic Charge Density

HCl		AN		ANHC		EB		ES	
Atom	**Charge**	**Atom**	**Charge**	**Atom**	**Charge**	**Atom**	**Charge**	**Atom**	**Charge**
$H_{1'}$	0.1854	N_1	-0.6560	N_1	-0.6761	N_1	-0.5322	N_1	-0.6152
$Cl_{2'}$	-0.1854	C_2	0.2745	C_2	0.2443	C_2	0.2274	C_2	0.2485
		C_3	-0.1131	C_3	-0.0976	C_3	-0.1009	C_3	-0.0973
		C_4	-0.0899	C_4	-0.0907	C_4	-0.0953	C_4	-0.0962
		C_5	-0.0958	C_5	-0.0850	C_5	-0.0838	C_5	-0.0777
		C_6	-0.0899	C_6	-0.0906	C_6	-0.0920	C_6	-0.0924
		C_7	-0.1131	C_7	-0.0981	C_7	-0.0883	C_7	-0.0917
		H_8	0.2547	H_8	0.2796	C_8	0.2664	C_8	0.3384
		H_9	0.2547	H_9	0.2802	C_9	-0.0816	C_9	-0.1044
				$H_{1'}$	0.1852	C_{10}	-0.0644	C_{10}	-0.0620
				$Cl_{2'}$	-0.2974	C_{11}	0.2702	C_{11}	0.2703
						C_{12}	-0.1092	C_{12}	-0.1026
						C_{13}	-0.0906	C_{13}	-0.0959
						N_{14}	-0.5497	N_{14}	-0.5351
						H_{15}	0.2256	H_{15}	0.2319
								$H_{1'}$	0.1870
								$Cl_{2'}$	-0.3252

Charge Density on Nitrogen

Two nitrogen atoms are present here N_1 and N_{14}, where N_1 and N_{14} are the bridging and terminal nitrogen atoms respectively. Charge on N_1 of ES is respectively 23.3 and 27 percentage lesser than that of AN and ANHC and 15.6% greater than EB. The similar trend is reflected on N_{14} of ES and the charge is only 2.7% greater than that of EB. Although charge density is inversely related to delocalisation, here the excess charge gained by N_1 and N_{14} of ES from the polymer chain enhance the conductance of ES as explained earlier.

Charge Density on Carbon

Significant carbon atoms chosen for the discussion are C_2, C_8 and C_{11}. All the carbon atoms are having positive charge. Both C_2 and C_8 have the similar trend of N_1 whereas meagre difference between ES and EB is observed for C_{11}.

3.3 Dipole moment

Dipole moment values are given in Table 3. Even though the total charge on a molecule is zero, the nature of chemical bonds is such that the positive and negative charges do not completely overlap in most molecules and this causes a permanent dipole moment. For polyatomic molecules there is more than one bond, and the total molecular dipole moment may be approximated as the vector sum of individual bond dipole moments. Dipole moment is used for the elucidation of structure of molecule, polarity of bonds, percentage ionic character and symmetry of molecule. Further it

explains the intermolecular interactions and other physical and chemical properties. Dipole moment measures the molecular polarizability as a whole as well as along the Cartesian coordinates.

Table 3: Dipole moment

	μ_x	μ_y	μ_z	μ_{Total}
HCl	0.0000	0.0000	-1.4335	1.4335
AN	-1.3012	-0.0001	-1.1067	1.7082
ANHC	3.4836	-0.5391	-3.0321	4.6497
EB	-1.6519	1.9196	0.5648	2.5947
ES	0.2417	6.3882	1.1098	6.4884
ES -Charge+1; Multiplicity- 2	-11.8146	2.2148	1.3340	12.0942

Total dipole moment of ES is 28.3 and 60 percentage higher than ANHC and EB and may account for the electrical conducting behaviour of ES. For EB and ES, the dipole moment along the *y*-axis is high when compared to other axes. This implies that the electron localisation is higher along the *y*-axis and which is also the direction of attack of the $H_{1'}$-$Cl_{2'}$ molecule. The $H_{1'}$-$Cl_{2'}$ molecule approaches AN along the *x*-axis, while for EB through *y*-axis. This may be due to the crowed *x* and *z*-axes of EB by steric and electronic effects of benzene ring. The second highest value of dipole moment for ES is along *z*-axis and this may make the polymer to transfer the polaron or charge carriers along the *yz*-plane through π-orbitals.

3.4 Molecular Orbital

MO theory is a method for determining molecular structure in which electrons are not assigned to individual bonds between atoms, but are treated as moving under the influence of the nuclei in the whole molecule. Frontier molecular orbital theory is an application of MO theory describing interactions of frontier orbitals HOMO/LUMO.

Fig 2 has the MO diagrams. For HCl the occupied MOs are highly spaced than the unoccupied MOs. In the case of AN, the unoccupied MOs are tightly bound than the unoccupied MOs of HCl. ANHC has the MOs of AN and HCl with slight destabilisation. MOs of AN and EB, ANHC and ES are comparable. Stability of HOMO of ES is -28.0, 19.6, -2.6, 2.5 percent changes from HCl, AN, ANHC and EB respectively. This infers that HCl is highly stable and ANHC is slightly stable than ES. Correspondingly for ES the LUMO is 2902.1, 1090.3, 30.6 and -31.0 % stable with respect to HCl, AN, ANHC and EB. As a result, the interaction between HCl and EB relatively changed the LUMO of ES over HOMO.
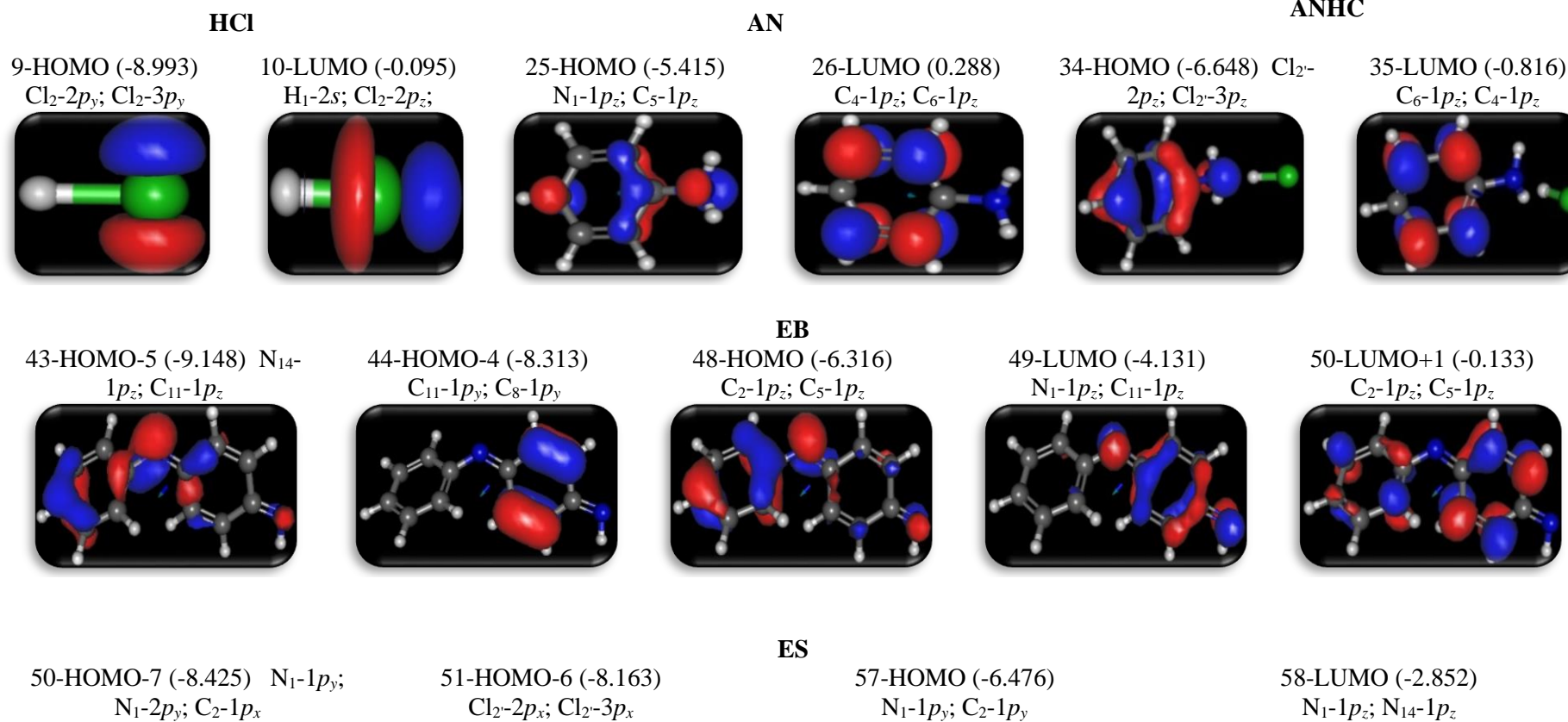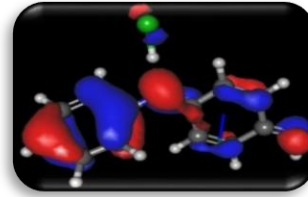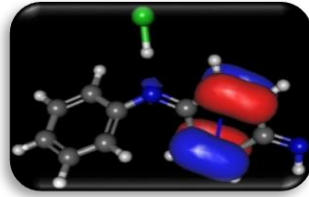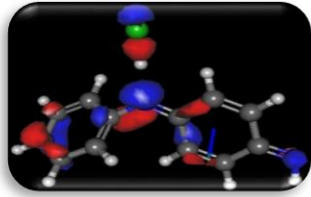
Figure 2: MO Diagram

HCl   AN   ANHC   EB   ES

Figure 2(a): MO Number, Name, Energy(eV) and AO Contribution to MO

HCl   **AN**   **ANHC**

9-HOMO (-8.993)   10-LUMO (-0.095)   25-HOMO (-5.415)   26-LUMO (0.288)   34-HOMO (-6.648) $Cl_{2'}$-   35-LUMO (-0.816)
Cl_2-$2p_y$; Cl_2-$3p_y$ H_1-$2s$; Cl_2-$2p_z$; N_1-$1p_z$; C_5-$1p_z$ C_4-$1p_z$; C_6-$1p_z$ $2p_z$; $Cl_{2'}$-$3p_z$ C_6-$1p_z$; C_4-$1p_z$

EB

43-HOMO-5 (-9.148) N_{14}-   44-HOMO-4 (-8.313)   48-HOMO (-6.316)   49-LUMO (-4.131)   50-LUMO+1 (-0.133)
$1p_z$; C_{11}-$1p_z$ C_{11}-$1p_y$; C_8-$1p_y$ C_2-$1p_z$; C_5-$1p_z$ N_1-$1p_z$; C_{11}-$1p_z$ C_2-$1p_z$; C_5-$1p_z$

ES

50-HOMO-7 (-8.425) N_1-$1p_y$;   51-HOMO-6 (-8.163)   57-HOMO (-6.476)   58-LUMO (-2.852)
N_1-$2p_y$; C_2-$1p_x$ $Cl_{2'}$-$2p_x$; $Cl_{2'}$-$3p_x$ N_1-$1p_y$; C_2-$1p_y$ N_1-$1p_z$; N_{14}-$1p_z$

3998

The nucleophilicity order is HCl > ANHC > ES > EB > AN and the order of electrophilicity is EB > ES > ANHC > HCl > AN. Thus, EB can react easily with HCl and forms ES. During the formation of ES, the electrons from the p_y orbital of $Cl_2$are shared with p_z orbital of N_1. For ES the HOMO is centred around ring A and LUMO is on ring B. Thus, the charge transport follows hoping mechanism.

3.5 Frontier Molecular Orbital

The values of the above parameters are given in Table 4. Band gap, is an energy range where no electron state can exist. It can be calculated form the difference between HOMO and LUMO [19]. The band gap based order of conductance is EB > ES > AN > ANHC > HCl. The difference in the experimental conductance value of ES and EB from the above computed order reveals the conductance in ES through polarons. Ionization potential (IP) is the energy necessary to remove an electron from the neutral atom and it often changes the molecular geometry [20]. The order of IP is; HCl > ANHC > ES > EB > AN. The IP values of ES and ANHC are comparable. The higher IP of ES over EB explains that, ES may be stable during the transport of electrons through it. Electron affinity is the amount of energy released when an electron is added to a neutral atom or molecule in the gaseous state to form a negative ion. The negative sign of electron affinity indicates to accept electron and vice versa. Except AN, all molecules can accept electrons readily and the order is EB > ES > ANHC > HCl > AN. This order confirms that EB can easily combine with HCl and gives ES.

Table 4: Frontier Molecular Orbital

	eV								Q^{Max}
	BG	**IP**	**EA**	**ECP**	**CH**	**GS**	**EI**	**EN**	
HCl	8.9	9.0	0.1	-4.5	4.4	0.2	45.9	4.5	1.0
AN	5.7	5.4	-0.3	-2.6	2.9	0.4	9.4	2.6	0.9
ANHC	5.8	6.6	0.8	-3.7	2.9	0.3	20.3	3.7	1.3
EB	1.9	6.0	4.1	-5.1	1.0	1.0	12.4	5.1	5.2
ES	3.6	6.5	2.9	-4.7	1.8	0.6	19.7	4.7	2.6
BG-Band Gap; IP-Ionisation Potential; EA-Electron Affinity; CH-Chemical Hardness; GS-Global Softness; EI-Elctrochmical Index; EN-Elctro Negativity									

Electronic chemical potential (ECP) is the quantity that measures the escaping tendency of electrons from a species in its ground state. It is the negative of the absolute electronegativity. It depends on the net charge of the atomic or molecular ions. The order of ECP/ reducing power is EB > ES > HCl > ANHC > AN. This order shows that electron cannoteasily escape from ES over EB and explain the former's conducting behaviour. HCl gets electrons from EB and forms ES voluntarily than the similar type of formation of ANHC. In HSAB concept of hard and soft for explaining stability of compounds, reaction mechanisms and pathways. Hard applies to species which are small, have high charge states and are weakly polarizable. Soft applies to species which are big, have low charge states and are strongly polarizable. The global softness and chemical hardness based reactivity order is EB > ES > AN ~ ANHC > HCl. The higher polarisable and chemical stability make EB less conducting than ES.

Electrophilic index is a measure of electrophilicity. The order of electron loving tendency is HCl > ANHC > ES > EB > AN. The lesser value of EB over ES may be attributed as, HCl and EB may have a molecular interaction instead of protonation. The absolute electronegativity, a measure of the tendency to attract bonded electrons follows the order EB > ES > HCl > ANHC > AN. The less electronegativity of ES over EB reveals that the electron localisation effect is higher in the later over former and accounts the conducting behaviour of the former. Q^{Max} is a measure of the number of transferable electrons which indicates that EB is electron rich over ES. Hence it has been concluded that there is a synergic interaction between HCl and polymer in ES. This study further confirms that

the conductance of ES is due to the mobility of proton between the quantum field produced by the EB and $Cl_{2'}$.

3.6 Docking studies

Docking is a measure of biological activities of a compound. Recent years the lung problem is a major one and here docking were done for SARS-CoV-2-7N0R. In order to get a clear understanding about PANI docking studies were done for AN, ANHC, EB and ES. The details are given in Table 5 and graphical representation is given by Fig.3.

Table 5: Docking studies

S.No.	Protein	Ligand	Binding affinity (kcal/mol)
1	7N0R	Aniline	-4.4
2	7N0R	Aniline HCl	-4.7
3	7N0R	EB	-6.5
4	7N0R	ES	-6.1

The binding order indicates that salts can bind the protein better than the neutral compound for the basic compounds AN and ANHC while the order is reversed for EB and ES. In ES the HCl is detached from the EB and indicate that PANI is a best carrier of drug and deliver in the spot by detaching the HCl form the EB in ES.

Figure 3: Docking studies

AN-7NOR

ANHC-7NOR

EB-7NOR

ES-7NOR
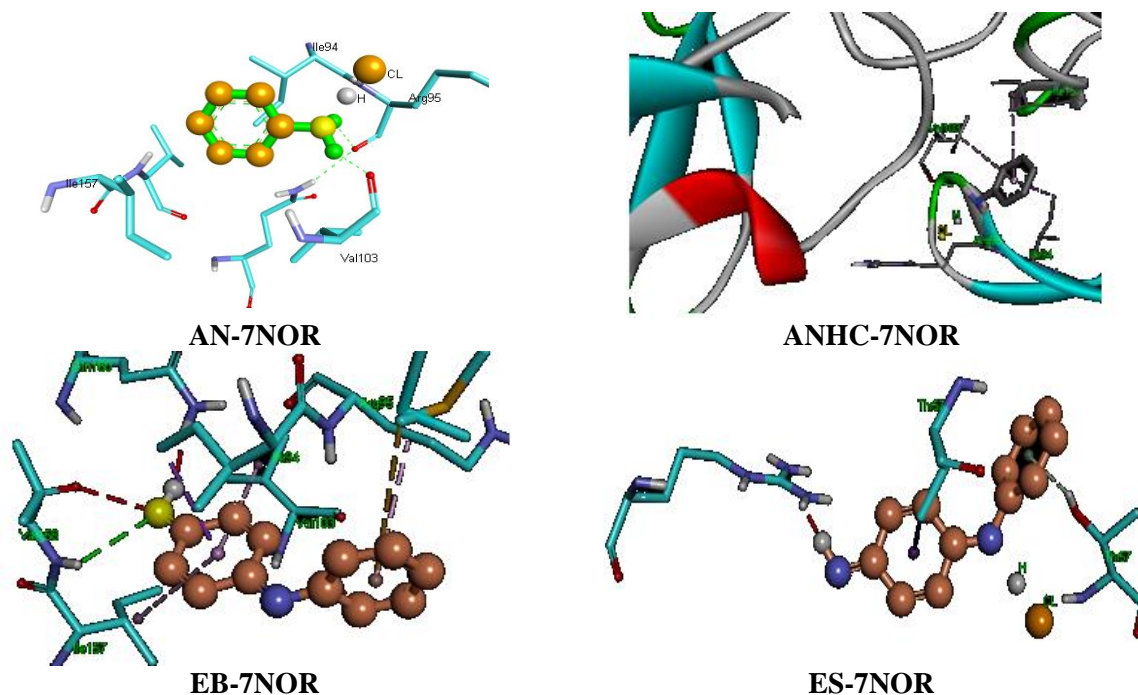
4. Conclusion

The conclusion derived from the study is the reaction between aniline and hydrochloride is equilibrium neutralization reaction. Three structures for aniline hydrochloride were fully optimized. In

4001

stable structure of aniline hydrochloride, aniline and HCl are each one H-bond acceptor and donor, where the acceptor is nitrogen and donor is chloride atoms. In aniline hydrochloride the HCl has free mobility throughout the whole volume of aniline at room temperature. ES (Charge=0; Mult=1) is the stable form among other multiplicities and charge. Stability of EB is less than aniline hydrochloride and ES. Reaction between EB and HCl is reversible neutralization. In ES, $H_{1'}$-$Cl_{2'}$ and polymer have synergic interaction. The charge carriers have hoping drift velocity through the time, space and energy dependent quantum field produced between $Cl_{2'}$ and polymer. Electronic, steric and isotropy effects play a major role in the conductance. The higher conductance of ES over EB is like the abnormal mobility of H^+ ion in liquids. Hence, ES is a solid solution of EB and HCl. The PANI can act as drug delivery system. Docking studies proved PANI has drug delivery polymer by its delocalised HCl group.

References

1. Elmowafy M., Shalaby, K., Elkomy, M.H., Alsaidan, O.A., Gomaa, H.A.M., Abdelgawad, M.A. and Mostafa, E.M., "Polymeric Nanoparticles for Delivery of Natural Bioactive Agents: Recent Advances and Challenges", *Polymers,* **2023**, 15, 1123.
2. Bassani D and Moro S., "Past, Present, and Future Perspectives on Computer-Aided Drug Design Methodologies", *Molecules*, **2023**, 28, 3906.
3. Sung, Y.K. and Kim, S.W., "Recent advances in polymeric drug delivery systems", *Biomater Res*, **2020,** 24, 12.
4. Le, T.-H., Kim, Y. and Yoon, H., "Electrical and Electrochemical Properties of Conducting Polymers", *Polymers*, **2017**, 9, 150.
5. Ke G, Chowdhury MH, Jin X and Li W., "Fabrication and properties of polyaniline/ramie composite fabric based on in situ polymerization", *Polymers and Polymer Composites*. **2021**, 29 (9_suppl), S914-S925.
6. Varghese, E. V., Thomas, B., Schwandt , C., Ramamurthy, P. C., and Joseph, A., "Benzimidazole-modified polyaniline micro-shells for electrochemical detection of cadmium in aqueous solution", *Journal of Electrochemical Science and Engineering*, **2023**, 13, 275–286.
7. Sumita Goswami, Suman Nandy, Elvira Fortunato and Rodrigo Martins, "Polyaniline and its composites engineering: A class of multifunctional smart energy materials", *Journal of Solid State Chemistry Part A,* **2023**, 317, 123679.
8. Kashyap G, Ameta G, Ameta C, Ameta R and Punjabi P.B, "Synthesis and characterization of polyaniline-drug conjugates as effective antituberculosis agents", "Bioorg Med Chem Lett." **2019**, 29, 1363-1369.
9. Jangid, Nirmala, Chauhan, Narendra Pal Singh, Meghwal, Kiran, Ameta, Rakshit, Punjabi, Pinki and Weaver, George, "Synthesis of dye-substituted polyanilines and study of their conducting and antimicrobial behavior", *Cogent Chemistry*, **2015**, 1, 1084666.
10. Chen X, Piao J, Dong H, Ou M, Lian R, Guan H, Cui J and Jiao C, "Organic Phosphoric Acid Doped Polyaniline-Coupled g-C_3N_4 for Enhancing Fire Safety of Intumescent Flame-Retardant Epoxy Resin", *Macromol Rapid Commun*. **2023**, e2300071.
11. Breijyeh Z, Jubeh B, and Karaman R., "Resistance of Gram-Negative Bacteria to Current Antibacterial Agents and Approaches to Resolve It", *Molecules*. **2020**, 25, 1340.
12. Nabi, S.A., Shahadat, Mohammad, Bushra, Rani, M., Oves and Ahmed, "Faheem, Synthesis and characterization of polyanilineZr(IV)sulphosalicylate composite and its applications (1) electrical conductivity, and (2) antimicrobial activity studies", *Chemical Engineering Journal*, **2011**, 173, 706.
13. Khairkar, Shyam and Raut, A, "Synthesis of Chitosan-graft-Polyaniline-Based Composites", *American Journal of Materials Science and Engineering*, **2014**, 2, 62-67.

14. Beygisangchin M, Abdul Rashid S, Shafie S, Sadrolhosseini A.R and Lim H.N, "Preparations, Properties, and Applications of Polyaniline and Polyaniline Thin Films-A Review", *Polymers* (*Basel*), **2021**, 13, 2003.

15. Sumita Goswami, Suman Nandy, Elvira Fortunato, and Rodrigo Martins, "Polyaniline and its composites engineering: A class of multifunctional smart energy materials", *Journal of Solid State Chemistry Part-A*, **2023**, 317, 123679.

16. Sholl, D.S and Steckel, "Density functional theory: a practical introduction", John Wiley & Sons, Hoboken, **2009**.

17. Granovsky, A.A Firefly version 8, www http://classic.chem.msu.su/gran/firefly/index.html; Schmidt, M.W Baldridge, K.K Boatz, J.A Elbert, S.T Gordon, M.S Jensen, J.H Koseki, S Matsunaga, N Nguyen, KA Su, S Windus, T.L Dupuis, M and Montgomery, J.A, "General atomic and molecular electronic structure system", *Journal of computational chemistry*, **1993**, 14, 1347-1363.

18. Jerome Eberhardt, Diogo Santos-Martins, Andreas F. Tillack, and Stefano Forl, *AutoDock Vina 1.2.0: New Docking Methods, Expanded Force Field, and Python Bindings", *J. Chem. Inf. Model.*, **2021**, 61, 8, 3891–3898.

19. Babu, V.S, "Solid state devices and technology*, Peason, New Delhi, 2010.

20. Cotton, FA and Wilkinson, G, Advanced inorganic chemistry, John Wiley, New Yor, 1988.